Fuel 290 (2021) 120080

Contents lists available at ScienceDirect

Fuel

journal homepage: www.elsevier.com/locate/fuel

Full Length Article

Machine learning assisted rediscovery of methane storage and separation in porous carbon from material literature

Chi Zhang [a,1], Dawei Li [a,1], Yunchao Xie [a], David Stalla [b], Peng Hua [c], Duy Tung Nguyen [d], Ming Xin [a], Jian Lin [a,c,d,e,*]

[a] Department of Mechanical and Aerospace Engineering, University of Missouri, Columbia, MO 65211, USA
[b] Electron Microscopy Core, University of Missouri, Columbia, MO 65211, USA
[c] Department of Biomedical, Biological and Chemical Engineering, University of Missouri, Columbia, MO 65211, USA
[d] Department of Physics and Astronomy, University of Missouri, Columbia, MO 65211, USA
[e] Department of Electrical Engineering and Computer Science, University of Missouri, Columbia, MO 65211, USA

ARTICLE INFO

Keywords:
Methane storage
Gas separation
Porous carbon
Machine learning
Literature mining

ABSTRACT

Porous carbon (PC) has been widely regarded as one of the most promising absorbents for methane storage. Studies show that its uptake capacity and selectivity highly depend on textural structures. Although much effort has been made, unveiling their detailed structure-performance relationship remains a challenge. Here, we propose an innovative study where, with the assistance of machine learning, the hidden relationship of the textural structures of PC with the methane uptake and separation can be derived from existing data in material literature. Machine learning models were trained by the data, including specific surface area, micropore volume, mesopore volume, temperature, and pressure as the input variables and methane uptake as the output variable for prediction. Among the tested models, the multilayer perceptron (MLP) shows the highest accuracy in predicting the methane uptake. In addition, the model enables to automatically construct a uptake performance map in terms of micropore volume and mesopore volume. The obtained MLP model was also extended to explore the CO_2/CH_4 selectivity by retraining it with the data collected from literature of PC for the CO_2 uptake. The constructed 2D selectivity map shows that the high selectivity can be achieved in the low CH_4 uptake region.

1. Introduction

As one of the most attractive clean fuels, natural gas (NG), consisting of >90% methane, is much cheaper than petroleum derived gasoline and diesel fuels [1]. Meanwhile, the high H/C ratio of methane betokens a high energy per mass as well as a high energy conversion efficiency [2]. Motivated by these advantages, methane has been successfully used as a vehicular fuel on a large scale [3]. However, its volumetric energy density under standard temperature and pressure conditions is only 0.12% of that of the gasoline, resulting in a very low mileage per unit volume of the tank. Thus, storage of adequate amount of NG in an onboard fuel tank remains a grand challenge. It can be usually solved by two possible strategies. One is to store NG under a high pressure (>20 MPa) or liquefy it under a low temperature (<112 K). The other one is to store it in porous sorbents at substantially lower pressures (3.5–6.5 MPa) and room temperature [4]. This strategy demands less energy and capital inputs, thus offering a more cost-effective and safer way to store NG at an acceptable gas density [5].

So far, various porous materials such as metal-organic framework (MOFs) [6] zeolites [7] organic polymer [8] and silicas [9] and activated carbons [10,11] have been intensively studied for methane storage. Among them, porous carbon (PC) has been widely regarded as one of the most promising absorbents due to its great uptake performance, low cost, facile production, and suitable textural structures [12–14]. Although much progress has been continuously made, deep understanding of the structure-performance relationship is still lacking, because their relationship is usually hidden in the high-dimensional data space. Delineation of such relationship calls for novel data analysis methods as well as provision of abundant high-quality data. However, usually, a very limited number of samples were synthesized, characterized and reported in each published paper. Such data deficiency would pose a challenge to unveil a comprehensive picture, although

* Corresponding author at: Department of Mechanical and Aerospace Engineering, University of Missouri, Columbia, MO 65211, USA.
E-mail address: linjian@missouri.edu (J. Lin).
[1] Equally contribute to the work.

https://doi.org/10.1016/j.fuel.2020.120080
Received 28 September 2020; Received in revised form 22 December 2020; Accepted 26 December 2020
Available online 8 January 2021

these papers may catch a glimpse on the relationship between the textural structures of PC and uptake performance. It is worth mentioning that so far hundreds of papers if not thousands have been published on this research topic. The accumulated data in these material literatures would offer a unique opportunity to fill this knowledge gap if a novel method can be developed.

In recent years, emerging data-driven methods based on statistics, machine learning (ML) has gained enormous attention in both industry and academy due to huge amount of accumulated data, continuously optimized algorithms, and exponential growth in computation capability [15]. Besides its applications in self-driving vehicles, image recognition and healthcare, ML has been rapidly introduced to the material science fields [16–18]. Recently, our group has successfully demonstrated that ML models can predict properties of 2D materials [19] perform inverse material design [20] assist material synthesis, extract chemical intuition from historic experimental data [21] and identify materials from their characterization data [22]. Despite the progress, to the best of our knowledge, using ML to disclose the quantitative relationship between the textural structures of PC and its CH_4 uptake performance has not been reported in literature. In addition, as the kinetic diameter and polarizability of CO_2 (3.30 Å, 26.3 × 10^{-25} cm^3 are quite close to those of CH_4 (3.80 Å, 26.0 × 10^{-25}) [23] using PC, a typical sorbent material, to separate CO_2 from CH_4 is still challenging. Although tuning the textural structures of PC is believed as a useful strategy to improve the CO_2/CH_4 selectivity [24] establishment of their relationship still relies on a trial-and-error process, which is time-consuming and very inefficient. Capability of ML in quantifying the relationship among different variables would make it potentially a new tool to study CO_2/CH_4 selectivity in PC.

Herein, without additional experimentation or simulation, we successfully demonstrated a ML based method to revisit methane uptake mechanism in PC by mining the data collected from published material literature. Contributions of this work can be summarized as follows. First, two well-trained ML models can accurately predict the CH_4 uptake of PC when specific surface area, micropore volume, mesopore volume serve as the input structural variables to train the models. Second, a structure-performance relationship map in terms of textural structures and CH_4 uptake is constructed via the assistance of ML models. This map would provide a direct tool for on-demand synthesis of next-generation PC for methane uptake. Third, the optimized multilayer perceptron (MLP) was further employed to provide new insights into the CO_2/CH_4 selectivity in PC. Finally, this innovative data-driven methodology offers a general platform for wide data extraction from material literature and intensive data exploration by the ML algorithms, which is invaluable to derive new knowledge for PC development, thus laying solid foundation for applications in supercapacitors [25] catalysis [26] and batteries [27] as well as for development of new advanced materials.

2. Methods

All MLPs were trained in the Python 3.7, Tensorflow 1.15.0 and Keras 2.3.1 environment. The MLP models for predicting the CH_4 and CO_2 uptake all consist of an input layer, three hidden layers, and an output layer (Fig. S1). The MLP model for predicting SSAs with V_{mi} and V_{me} as the input variables consists of an input layer, three hidden layers with 64, 32 and 16 neurons, respectively, and an output layer. The epoch for training all the MLP models was set as 1000. 1774 datasets for the CH_4 uptake were collected from 40 previously published papers (Table S1), while 1020 datasets for the CO_2 uptake were referenced to the previous work [28]. In general, all these data collected for CH_4 and CO_2 is based on pure carbon without heteroatom N doping, since N has proved to have great influence on the gas adsorption and separation, especially for CH_4 [29] and CO_2 [30,31]. These datasets were randomly split to training and testing sets with a ratio of 4:1 for five times. All ML models were trained on the training datasets, and performance was evaluated on the testing set. After the training was finished, evaluation metrics were summarized in Table S3. Details about the remaining four ML models that were used in this study can be found in SI.

3. Results and discussion

Fig. 1a shows the flow chart of exploring the structure–performance relationship of PC with the assistance of ML *via* mining the material literature. Based on existing scientific understanding, we first identified a total of 5 input features, or called the chemical descriptors, which may govern the uptake performance of CH_4. In addition to temperature (T) and pressure (P), three textural structures including specific surface area (SSA), micropore volume (V_{mi}), and mesopore volume (V_{me}) are also taken into account. Previous studies have proved that these textural structures have great influence on the CH_4 storage capacity [32,33]. Meanwhile, the corresponding CH_4 uptake serves as the output prediction of the models. In this work, a total of 1974 experimentation datapoints including input and output data were mined from tables and adsorption isotherms in 40 papers to build a database. All these extracted data is based on pure porous carbon, since nitrogen doping has been proven to affect the gas uptake and selectivity [30]. Meanwhile, these papers cover PCs produced from various precursors and by various fabrication methods (Table S1). In addition, the produced PCs possess a wide range of textural characteristics (Fig. S2), while, the frequency distribution of methane uptake is shown in Fig. S3. The histogram in Fig. S3 depicts that methane uptake has right-skewed distribution. Then, all the datasets were first randomly shuffled and split into training and testing datasets with a ratio of 4:1 (Fig. S4). Then, the training datasets were standardized to rescale the range of inputs within 0 and 1. After that, a series of widely used ML models, including random forest (RF), support vector machine (SVM), elastic network (EN), least absolute

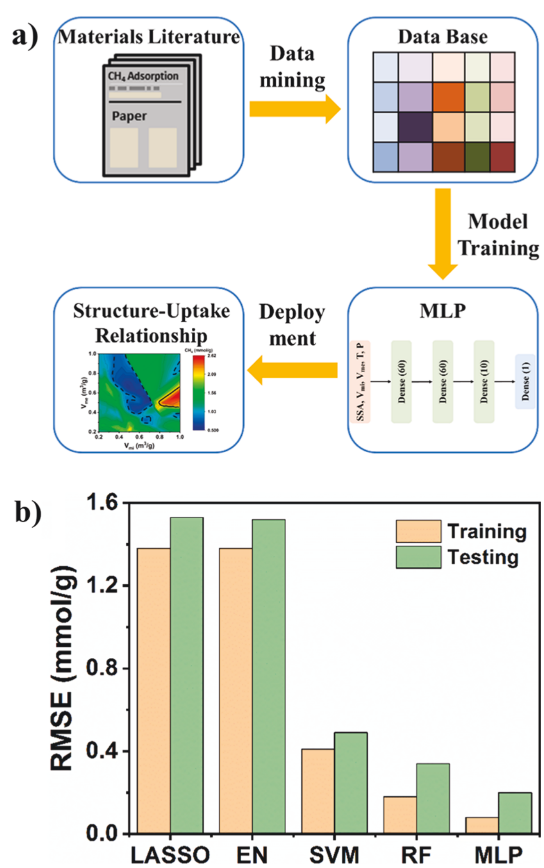

Fig. 1. (a) A flow chart of exploring the structure–performance relationship of PC for methane storage and separation by mining data from material literature. (b) RMSEs of predicted CH_4 uptake from various ML models.

shrinkage and selection operator (LASSO), and MLP were trained. The objective of investigating various ML models is to find a model with the highest prediction accuracy. Their hyperparameters after these models were tested and optimized were summarized in Table S2. Detailed explanation of these ML models can be found in Supporting Information. The evaluation metrics including root-mean-square error (RMSE), mean absolute error (MAE) and mean absolute percentage error (MAPE) were calculated from these models and summarized in Table S3. Here, RMSE was adopted to compare different models due to its capability of reflecting prediction accuracy. As shown in Fig. 1b, RF and MLP generate relatively smaller RMSEs in both training and testing datasets, indicating that both models outperform others in predicting the CH_4 uptake of PC.

These two models, RF and MLP, which provided the second highest and the highest prediction accuracy, respectively, were further compared. Fig. 2a-b show that both models exhibit strong linear correlation between the predicted values (N_{pv}) and experimental ones (N_{ev}). The correlation factors (R^2) of testing data and the predicted values from the RF and MLP models are both 0.99. As quantitative evaluation and comparison, the relative error between N_{pv} and $N_{ev,}$ was calculated as $|N_{pv} - N_{ev}|/N_{ev}$. As shown in Fig. 2c-d, compared with RF which generates possibility of ~57% when predicting methane uptake within a relative error of < 10%, MLP offers a higher possibility of ~75% to achieve the same prediction error. This number increases to ~90% if the predicted uptake is within a relative error of 20%. This high prediction accuracy provided by both models indicates that the selected input features are reasonable for model development, and they all affect the uptake to some extent.

In order to disclose the role of SSA, V_{mi} and V_{me}—the features that are closely related to the intrinsic physical properties of PC—in determining the CH_4 uptake, quantification of the relative importance of each input is necessary, while it is still challenging to be achieved *via* traditional analysis methods. It should be noted that most ML algorithms including MLP have difficulty in providing an explanation of the predicted results owing to their so-called "black-box" nature [21]. But, the decision tree based ones, like RF, provide an out-of-box method that can export the weight of each input feature in determining the output prediction [34]. As shown in Fig. 3, among the three structural features, SSA is the dominant one in determining the CH_4 uptake. This result is well accepted in the field [35]. For example, Gu *et al.* found that a larger SSA is favorable to CH_4 uptake after studying adsorption properties of a series of granular activated carbons with similar properties but different pore structures [36]. In addition, it has been shown that for small gas molecules (e.g. CH_4), absorption mainly takes place in the micropores [29]. This conclusion is also supported by the result shown in Fig. 3, which indicates that V_{mi} is the second dominant factor that contributes greatly to the CH_4 uptake [37,38].

Another power of the ML algorithms is that they can generate new data by learning the patterns formed by the historic data. These newly generated data can cover the data points which are not reported in previous experiments. By this way, a comprehensive contour map that shows the methane uptake as a function of the corresponding textural structures can be obtained to further elucidate the structure-uptake

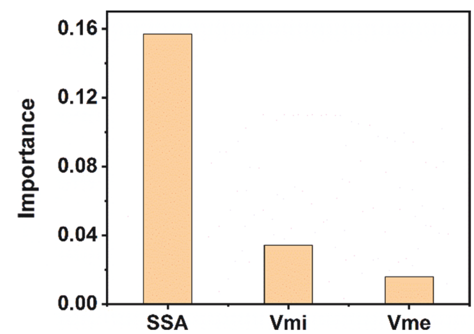

Fig. 3. Feature importance of each input descriptor derived from the RF model.

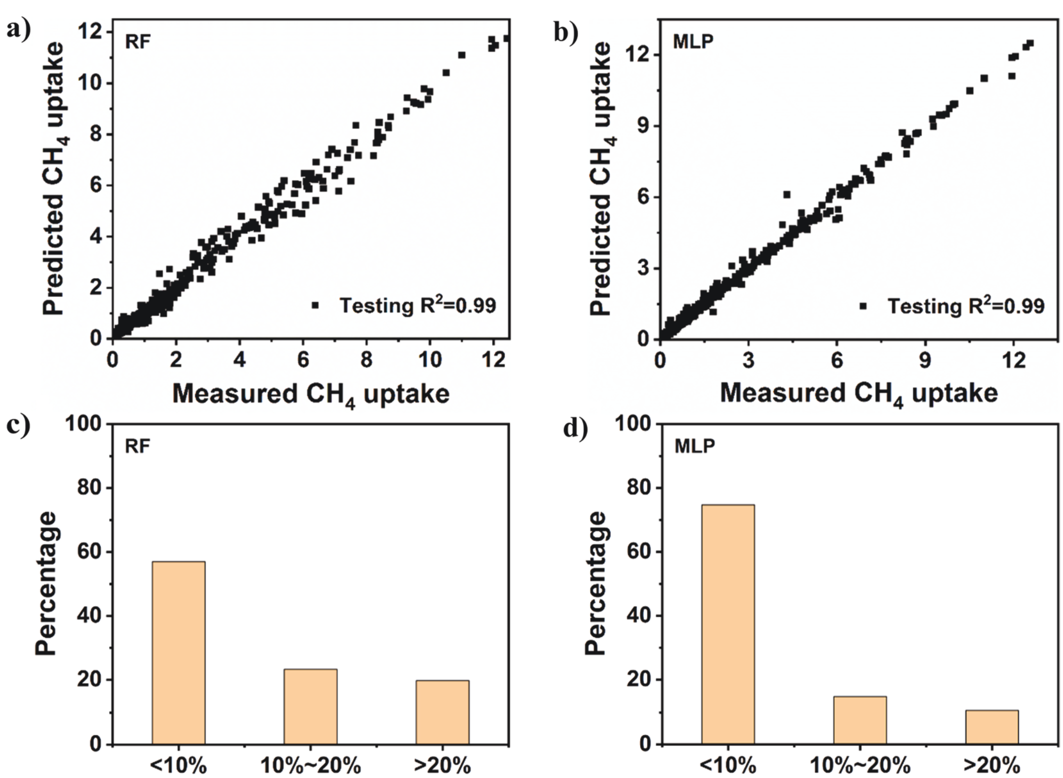

Fig. 2. Measured data of CH_4 uptake vs. predicted uptake value from two ML models: (a) RF and (b) MLP. The unit is mmol/g for the uptake. Error distribution of predicted CH_4 uptake values from two ML models: (c) RF and (d) MLP.

relationship. In other words, this map can not only explicitly show the effect of individual textural structure of PC on the CH_4 uptake, but also reveal the optimized PC structures. However, it is possible that the models may also generate some data points with extreme values that are contradictory to real situations, for instance, a high SSA with almost zero V_{mi} and V_{me} [39]. Therefore, prior to the map construction, we explored the possibility to reduce the input feature SSA. Herein, we trained another MLP model that can predict the SSA with given experimental V_{mi} and V_{me} ranging from 0.2 to 1 cm^3/g. As SSA is closely related to V_{mi} and V_{me}, we expect that the model trained with experimentally obtained V_{mi} and V_{me} would result in reasonable SSA. The predicted SSA vs. the testing SSA is shown in Fig. S5a. High R^2 of 0.81 for the testing dataset suggests that SSA has strong correlation with V_{mi} and V_{me}. Fig. S5b shows a contour map of predicted SSA as a function of V_{mi} and V_{me}. As expected, the high SSA appears in the region enclosed by large V_{mi} and V_{me}. For instance, when V_{mi} is 1.0 cm^3/g, increase of V_{me} from 0.2 cm^3/g to 1.0 cm^3/g results in the increase of SSA from ~2454 m^2/g to ~3168 m^2/g. These results suggested that SSA as an input feature for predicting CH_4 uptake could be reduced, as its information could be indirectly reflected by V_{mi} and V_{me}.

Then we retrained the MLP model for CH_4 uptake with only V_{mi}, V_{me}, T and P as input features. As we expect, it stills shows a good linear relationship between predicted value and measured one (Fig. S6a), although, the prediction accuracy of retrained model is not as good as the one with SSA as input features due to the input feature reduction (Fig. S6b). It provides an opportunity to reflect the CH_4 uptake in terms of V_{mi} and V_{me} under specific T and P. Then, we generated a series of different hypothetical combinations of V_{mi} and V_{me} ranging from 0.2 to 1.0 cm^3/g. After that the retained MLP is used to predict the corresponding CH_4 uptake value to further construct the performance maps at 25 °C under pressures of 1 bar, 5 bar, 10 bar and 20 bar, respectively as shown in Fig. 4. At 1 bar, the highest CH_4 uptake (2.6 mmol/g) appears in a region enclosed by large V_{mi} (0.82 ~ 1 cm^3/g) and medium V_{me} (0.51 ~ 0.64 cm^3/g) (Fig. 4a). This result is in good agreement with previous studies showing that the CH_4 uptake is primary governed by V_{mi} under ambient conditions [40]. As the pressure increases, the distribution of CH_4 uptake region is varied. For instance, when the pressure is elevated to 5 bar, the area of high uptake region increases and moves. Specifically, V_{mi} and V_{me} shift to 0.6 ~ 0.95 cm^3/g and 0.47 ~ 1 cm^3/g, respectively. Our findings are in consistent with the experimental observation that hierarchical porous carbon has higher gas adsorption than microporous carbon does at high pressure [41]. Similarly, Cai *et al.* analyzed a series of porous carbon and concluded that mesopore also contributes the CH_4 uptake at elevated pressure due to the condensation effect [35]. It is also believed that the existence of mesopores can facilitate the diffusion of the gas molecules into the micropores at high pressure, leading to the enhancement of the CH_4 adsorption [42]. Meanwhile, the area of region corresponding to low methane uptake moved to low V_{mi} and low V_{me} region, as marked by dash lines in Fig. 4b. However, such a distribution change for high uptake region becomes less prominent as the pressure is further increased. As shown in Fig. 4c, when the pressure is further increased to 10 bar, the high methane uptake region is enclosed by V_{mi} of 0.54 ~ 0.81 cm^3/g and V_{me} of 0.64 ~ 1 cm^3/g, which is similar to the one obtained at 5 bar. Meanwhile, it should be noted that another region with V_{mi} of 0.54 ~ 0.65 cm^3/g and V_{me} of 0.55 ~ 0.77 cm^3/g corresponding to high uptake at 5 bar changed into moderate uptake when pressure is at 10 bar. This trend continues as the pressure is further elevated to 20 bar, the resulting distribution of high and moderate uptake regions (Fig. 4d) are almost as the same as the ones shown in Fig. 4c. Furthermore, from the derived performance map the effect of V_{me} on the CH_4 uptake is further disclosed that V_{me} plays a more and more important role in contributing the CH_4 uptake as pressure increases. For instance, if the uptake of PC with V_{mi} of 0.65 cm^3/g is measured at 20 bar (Fig. 4d), the increase of V_{me} from 0.2 cm^3/g to 1 cm^3/g increases the uptake capacity from 7 mmol/g to 11.4 mmol/g. While, no matter under what pressures, a relatively high V_{mi} (>0.6 $cm^3/$

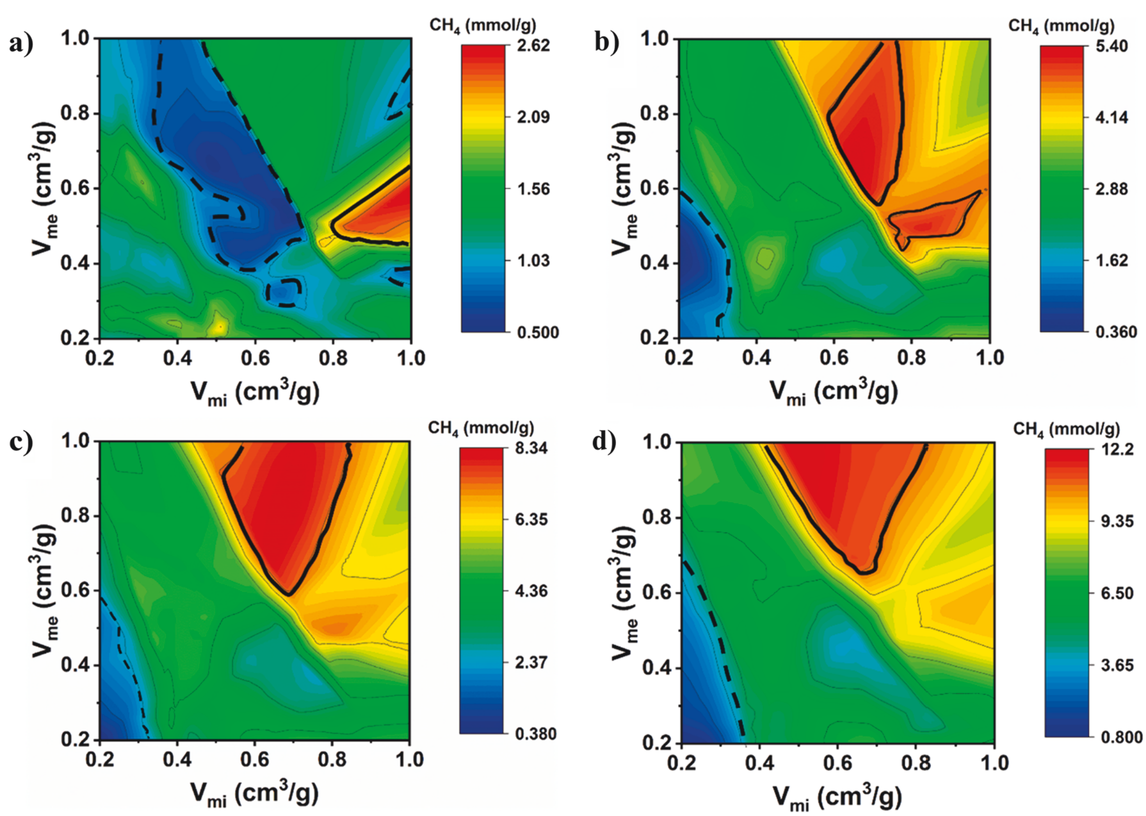

Fig. 4. Contour maps of CH_4 adsorption capacities (mmol/g) as functions of V_{mi} and V_{me} at 25 °C and 1 bar (a), 5 bar (b), 10 bar (c) and 20 bar (d), respectively. The high and low uptake regions are enclosed by solid and dash lines, respectively.

g) is always needed to achieve a high uptake capacity. This result is in line with the result shown in Fig. 3 that V_{mi} is more important than V_{me}.

This methodology enabled by the ML models offers a new avenue to reveal the correlation between textural structures of pristine PC and their corresponding CH_4 uptake. Such success inspires us to look into other gases, e.g. CO_2, with a goal of studying the gas selectivity of PC for CH_4 and CO_2 separation. With the same input descriptors (V_{mi}, V_{me}, T and P) and 1020 datasets collected from a previous work [28] a MLP model trained for a CO_2 uptake results in a high prediction accuracy with R^2 of 0.99 for the testing dataset (Fig. S6c). The error distribution of these predicted CO_2 uptake values shows that >55% of predicted values has <10% of relative errors (Fig. S6d). The accuracy can be further improved with the size of database increases. By following the same procedure of obtaining Fig. 4, a performance map showing the relation of the CO_2 uptake performance as a function of V_{mi} and V_{me} at 1 bar was constructed (Fig. 5a). It shows that the maximum CO_2 uptake (4.5 mmol/g) appears in a region enclosed by high V_{mi} ($0.65 \sim 0.88$ cm^3/g) and medium V_{me} ($0.2 \sim 0.4$ cm^3/g), which is in a good agreement with previous studies [28,43]. For example, Zhang *et al.* reported that micropores are preferred for achieving high CO_2 adsorption at ambient conditions [28]. Moreover, Govind Sethia *et al.* synthesized a series of strictly microporous nitrogen doped activated carbon and found that micropores, especially ultra-micropores has a significant impact on the CO_2 adsorption [43].

Then by assuming a 50:50 mixture of CO_2/CH_4, a typical volume ratio in landfill gas, the selectivity map was calculated based on the ideal absorbed solution theory (IAST) [44]. The IAST-derived selectivity is defined by using the equation of $S_{CO2/CH4} = (n_{CO2}/p_{CO2})/(n_{CH4}/p_{CH4})$, where n_{CO2} and n_{CH4} are the predicted CO_2 uptake and CH_4 uptake at 0.5 bar and at 0.5 bar, respectively. n_{CO2} and n_{CH4} are directly obtained from Fig. 5b-c. Fig. 5d shows the corresponding calculated selectivity map. And it shows that the region with the highest selectivity (>5) is enclosed by V_{mi} in the range from 0.63 to 0.72 cm^3/g and V_{me} in the range from 0.5 to 0.6 cm^3/g which is also located in the region corresponding to low CH_4 uptake region as shown in Fig. 5b. Such result indicates that the high selectivity region is determined by the low CH_4 uptake region instead of high CO_2 uptake region, which elucidates the direction of potential interest for future experimental synthesis. Fig. 5 also suggests that a high V_{mi} of microporous carbon may not favor the separation of the CO_2/CH_4 gas mixtures at atmospheric pressure which agrees well with a recent experiment study [45]. In that work, they systematically investigated the roles of pore characteristics in terms of SSA, V_{mi} and V_{me} on the separation of CO_2/CH_4. They found that at atmospheric pressure, high SSA and V_{mi} led to relative low separation efficiency. In contrast, mesopores promoted the gas separation. Such effect is more profound when pressure increases [45]. It is worth mentioning that this positive role of mesopore in gas separation has also been reported in CO_2/N_2 gas mixtures [46].

4. Conclusion

In summary, a general platform of ML algorithms for mining data from material literature was developed to revisit methane uptake mechanism and selectivity in PC. The well-trained ML models enable the prediction of methane uptake and offer new data for constructing performance and selectivity maps that help to unveil the underlying structure-performance relationship. They not only offer high prediction accuracy but also disclose a clear role of V_{me} in the CH_4 uptake, which is obtained by the data-driven approach. Moreover, we found that the textural structures of pristine PC with the high CO_2 and CH_4 uptake lead to moderate CO_2/CH_4 selectivity. To achieve a CO_2/CH_4 selectivity of > 5, synthesis of PC with suitable textural structures is essential and doable. Such rediscovered knowledge is beneficial to future development of advanced PC for gas absorption and separation. Finally, this ML

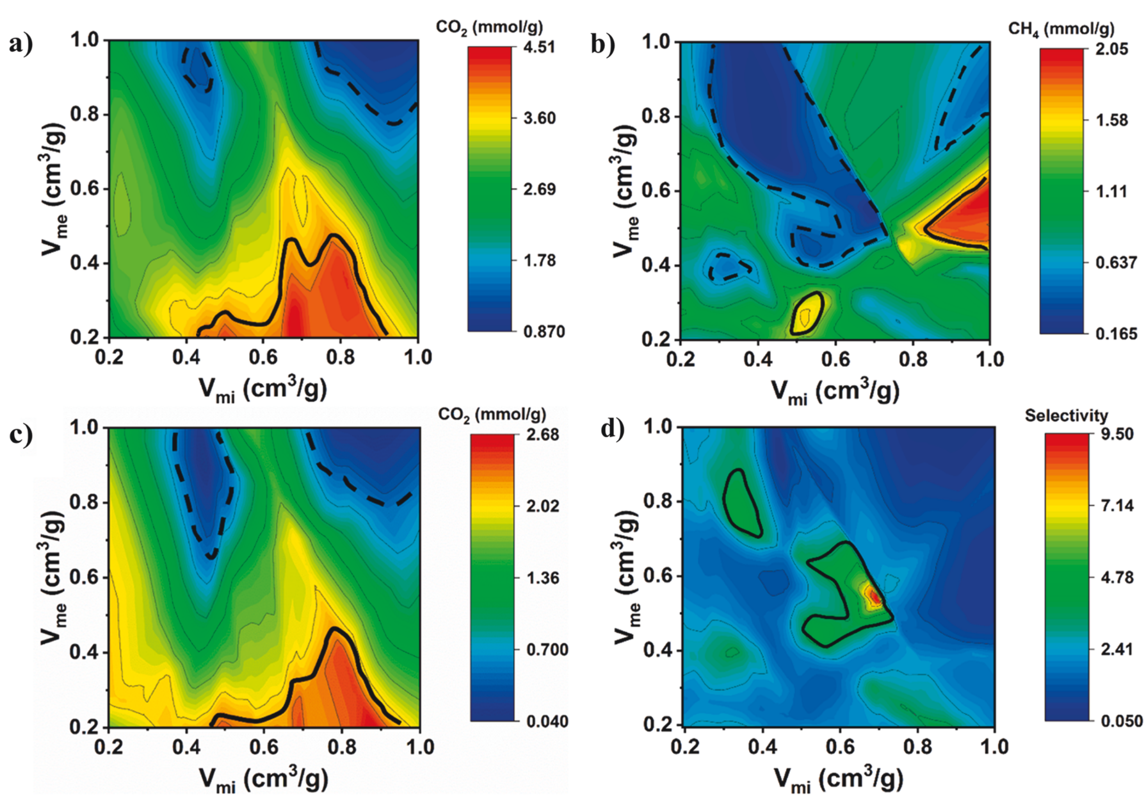

Fig. 5. (a) A contour map of CO_2 uptake as a function of V_{mi} and V_{me} at 25 °C and 1 bar. The high and low uptake regions are enclosed by solid and dash lines, respectively. Contour maps of CH_4 (b) and CO_2 uptake (c) as a function of V_{mi} and V_{me} at 25 °C and under 0.5 bar and 0.5 bar, respectively. The high and low uptake regions are enclosed by solid and dash lines, respectively. (d) A CO_2/CH_4 selectivity map in porous carbon at 25 °C and 1 bar. The regions with high selectivity are enclosed by solid lines.

assisted methodology can be extended to other applications of PC such as energy storages and conversion and applied to develop new advanced materials.

CRediT authorship contribution statement

Chi Zhang: Conceptualization, Methodology, Investigation, Formal analysis, Data curation, Writing - original draft. **Dawei Li:** Methodology, Software, Writing - review & editing. **Yunchao Xie:** Methodology, Software, Writing - review & editing. **David Stalla:** Investigation, Formal analysis. **Peng Hua:** . **Duy Tung Nguyen:** . **Ming Xin:** Methodology, Supervision. **Jian Lin:** Conceptualization, Methodology, Investigation, Supervision, Project administration, Writing - review & editing.

Declaration of Competing Interest

The authors declare that they have no known competing financial interests or personal relationships that could have appeared to influence the work reported in this paper.

Acknowledgments

This work was financially supported by grants from National Science Foundation (award number: 1825352 and 1933861), United States Department of Energy National Energy Technology Laboratory (award number: DE-FE0031645), and United States Department of Agriculture (award number: 2018-67017-27880 and 2020-67030-31336).

Appendix A. Supplementary data

Supplementary data to this article can be found online at https://doi.org/10.1016/j.fuel.2020.120080.

References

[1] Lozano-Castelló D, Alcañiz-Monge J, de la Casa-Lillo MA, Cazorla-Amorós D, Linares-Solano A. Advances in the study of methane storage in porous carbonaceous materials. Fuel 2002;81(14):1777–803.
[2] Casco ME, Martínez-Escandell M, Gadea-Ramos E, Kaneko K, Silvestre-Albero J, Rodríguez-Reinoso F. High-pressure methane storage in porous materials: are carbon materials in the pole position? Chem Mater 2015;27(3):959–64.
[3] Menon VC, Komarneni S. Porous adsorbents for vehicular natural gas storage: a review. J Porous Mater 1998;5(1):43–58.
[4] Choi S, Alkhabbaz MA, Wang Y, Othman RM, Choi M. Unique thermal contraction of zeolite-templated carbons enabling micropore size tailoring and its effects on methane storage. Carbon 2019;141:143–53.
[5] Chen Z, Li P, Anderson R, Wang X, Zhang X, Robison L, et al. Balancing volumetric and gravimetric uptake in highly porous materials for clean energy. Science 2020;368(6488):297–303.
[6] Peng Y, Krungleviciute V, Eryazici I, Hupp JT, Farha OK, Yildirim T. Methane storage in metal–organic frameworks: current records, surprise findings, and challenges. J Am Chem Soc 2013;135(32):11887–94.
[7] Cavenati S, Grande CA, Rodrigues AE. Adsorption equilibrium of methane, carbon dioxide, and nitrogen on zeolite 13X at high pressures. J Chem Eng Data 2004;49(4):1095–101.
[8] Wood CD, Tan B, Trewin A, Su F, Rosseinsky MJ, Bradshaw D, et al. Microporous organic polymers for methane storage. Adv Mater 2008;20(10):1916–21.
[9] Saini VK, Andrade M, Pinto ML, Carvalho AP, Pires J. How the adsorption properties get changed when going from SBA-15 to its CMK-3 carbon replica. Sep Purif Technol 2010;75(3):366–76.
[10] Wu Y-J, Yang Y, Kong X-M, Li P, Yu J-G, Ribeiro AM, Rodrigues AE. Adsorption of Pure and Binary CO_2, CH_4, and N_2 Gas Components on Activated Carbon Beads. J Chem Eng Data 2015;60(9):2684–93.
[11] Kumar KV, Preuss K, Titirici M-M, Rodríguez-Reinoso F. Nanoporous materials for the onboard storage of natural gas. Chem Rev 2017;117(3):1796–825.
[12] Jalilov AS, Ruan G, Hwang C-C, Schipper DE, Tour JJ, et al. Asphalt-derived high surface area activated porous carbons for carbon dioxide capture. ACS Appl Mater Interfaces 2015;7(2):1376–82.
[13] Tang R, Dai Q, Liang W, Wu Y, Zhou X, Pan H, et al. Synthesis of novel particle rice-based carbon materials and its excellent CH_4/N_2 adsorption selectivity for methane enrichment from Low-rank natural gas. Chem Eng J 2020;384:123388. https://doi.org/10.1016/j.cej.2019.123388.
[14] Jalilov AS, Li Y, Tian J, Tour JM. Ultra-high surface area activated porous asphalt for CO_2 capture through competitive adsorption at high pressures. Adv Energy Mater 2017;7(1):1600693.
[15] Schmidt J, Marques MRG, Botti S, Marques MAL. Recent advances and applications of machine learning in solid-state materials science. NPJ Comput Mater 2019;5(1):83.
[16] Tabor DP, Roch LM, Saikin SK, Kreisbeck C, Sheberla D, Montoya JH, et al. Accelerating the discovery of materials for clean energy in the era of smart automation. Nat Rev Mater 2018;3(5):5–20.
[17] Butler KT, Davies DW, Cartwright H, Isayev O, Walsh A. Machine learning for molecular and materials science. Nature 2018;559(7715):547–55.
[18] Tshitoyan V, Dagdelen J, Weston L, Dunn A, Rong Z, Kononova O, et al. Unsupervised word embeddings capture latent knowledge from materials science literature. Nature 2019;571(7763):95–8.
[19] Dong Y, Wu C, Zhang C, Liu Y, Cheng J, Lin J. Bandgap prediction by deep learning in configurationally hybridized graphene and boron nitride. NPJ Comput Mater 2019;5(1):26.
[20] Dong Y, Li D, Zhang C, Wu C, Wang H, Xin M, et al. Inverse design of two-dimensional graphene/h-BN hybrids by a regressional and conditional GAN. Carbon 2020;169:9–16.
[21] Xie Y, Zhang C, Hu X, Zhang C, Kelley SP, Atwood JL, et al. Machine learning assisted synthesis of metal–organic nanocapsules. J Am Chem Soc 2020;142(3):1475–81.
[22] Wang H, Xie Y, Li D, Deng H, Zhao Y, Xin M, et al. Rapid Identification of X-ray Diffraction Patterns Based on Very Limited Data by Interpretable Convolutional Neural Networks. J Chem Inf Model 2020;60(4):2004–11.
[23] Jalilov AS, Li Y, Kittrell C, Tour JM. Increased CO_2 selectivity of asphalt-derived porous carbon through introduction of water into pore space. Nat Energy 2017;2(12):932–8.
[24] Tour JM, Schipper DE, Hwang C-C, Tour J, Jalilov AS, Ruan G, et al. Porous carbon materials for CO_2 separation in natural gas. Google Patents 2017.
[25] Li L, Zhong Q, Kim ND, Ruan G, Yang Y, Gao C, et al. Nitrogen-doped carbonized cotton for highly flexible supercapacitors. Carbon 2016;105:260–7.
[26] Zhang C, Xie Y, Deng H, Zhang C, Su J, Lin J. Nitrogen doped coal with high electrocatalytic activity for oxygen reduction reaction. Eng. Sci. 2019:39–45.
[27] Luong DX, Bets KV, Algozeeb WA, Stanford MG, Kittrell C, Chen W, et al. Gram-scale bottom-up flash graphene synthesis. Nature 2020;577(7792):647–51.
[28] Zhang Z, Schott JA, Liu M, Chen H, Lu X, Sumpter BG, et al. Prediction of Carbon Dioxide Adsorption via Deep Learning. Angew Chem 2019;131(1):265–9.
[29] Pan H, Yi Y, Lin Q, Xiang G, Zhang Yu, Liu F. Effect of surface chemistry and textural properties of activated carbons for ch 4 selective adsorption through low-concentration coal bed methane. J Chem Eng Data 2016;61(6):2120–7.
[30] Saha D, Kienbaum MJ. Role of oxygen, nitrogen and sulfur functionalities on the surface of nanoporous carbons in CO2 adsorption: A critical review. Microporous Mesoporous Mater 2019;287:29–55.
[31] Wang L, Yang RT. Significantly increased CO_2 adsorption performance of nanostructured templated carbon by tuning surface area and nitrogen doping. J Phys Chem C 2012;116(1):1099–106.
[32] Lozano-Castelló D, Cazorla-Amorós D, Linares-Solano A, Quinn DF. Influence of pore size distribution on methane storage at relatively low pressure: preparation of activated carbon with optimum pore size. Carbon 2002;40(7):989–1002.
[33] Luo J, Liu Y, Jiang C, Chu W, Jie W, Xie H. Experimental and Modeling Study of Methane Adsorption on Activated Carbon Derived from Anthracite. J Chem Eng Data 2011;56(12):4919–26.
[34] Chen T, Xgboost GC. A scalable tree boosting system. In: Proceedings of the 22nd ACM SIGKDD International Conference on Knowledge Discovery and Data Mining; 2016. p. 785–94.
[35] Cai J, Qi J, Yang C, Zhao X. Poly(vinylidene chloride)-Based Carbon with Ultrahigh Microporosity and Outstanding Performance for CH_4 and H_2 Storage and CO_2 Capture. ACS Appl Mater Interfaces 2014;6(5):3703–11.
[36] Gu M, Zhang B, Qi Z, Liu Z, Duan S, Du X, et al. Effects of pore structure of granular activated carbons on CH_4 enrichment from $C_H4/_N2$ by vacuum pressure swing adsorption. Sep Purif Technol 2015;146:213–8.
[37] Zhao J, Wei J, Cai D, Cao H, Tan T. Polyaspartic acid-derived micro-/mesoporous carbon for ultrahigh H_2 and CH_4 Adsorption. ACS Omega 2020;5(19):10687–95.
[38] Yuan B, Wu X, Chen Y, Huang J, Luo H, Deng S. Adsorption of CO_2, CH_4, and N_2 on ordered mesoporous carbon: approach for greenhouse gases capture and biogas upgrading. Environ Sci Technol 2013;47(10):5474–80.
[39] Wang S, Zhang Z, Dai S, Jiang D-E. Insights into CO_2/N_2 Selectivity in Porous Carbons from Deep Learning. ACS Materials Lett. 2019;1(5):558–63.
[40] Li Y, Li D, Rao Y, Zhao X, Wu M. Superior CO_2, CH_4, and H_2 uptakes over ultrahigh-surface-area carbon spheres prepared from sustainable biomass-derived char by CO_2 activation. Carbon 2016;105:454–62.
[41] Travis W, Gadipelli S, Guo Z. Superior CO 2 adsorption from waste coffee ground derived carbons. RSC Adv. 2015;5(37):29558–62.
[42] Peredo-Mancilla D, Ghouma I, Hort C, Ghimbeu CM, Jeguirim M, Bessieres D. CO2 and CH4 Adsorption Behavior of Biomass-Based Activated Carbons. Energies 2018;11(11):3136.
[43] Sethia G, Sayari A. Comprehensive study of ultra-microporous nitrogen-doped activated carbon for CO_2 capture. Carbon 2015;93:68–80.

[44] Myers AL, Prausnitz JM. Thermodynamics of mixed-gas adsorption. AIChE J 1965;11(1):121–7.

[45] Yi H, Li Y, Tang X, Li F, Li K, Yuan Q, Sun X. Effect of the adsorbent pore structure on the separation of carbon dioxide and methane gas mixtures. J Chem Eng Data 2015;60(5):1388–95.

[46] Lee JH, Lee HJ, Lim SY, Kim BG, Choi JW. Combined CO_2 -philicity and ordered mesoporosity for highly selective CO_2 capture at high temperatures. J Am Chem Soc 2015;137(22):7210–6.